Regulation of Dendritic Maintenance and Growth by a Mammalian 7-Pass Transmembrane Cadherin

Yasuyuki Shima,[1,2,6] Mineko Kengaku,[2,4,5]
Tomoo Hirano,[2,4] Masatoshi Takeichi,[3]
and Tadashi Uemura[1,4,6,*]
[1]Department of Molecular Genetics
The Institute for Virus Research
[2]Department of Biophysics
Graduate School of Science
Kyoto University
Kyoto 606-8507
Japan
[3]RIKEN Center for Developmental Biology
2-2-3 Minatojima-Minamimachi
Chuo-ku, Kobe 650-0047
Japan
[4]Core Research for Evolutional Science
    and Technology (CREST)
Japan Science and Technology Agency
Kawaguchi, Saitama 332-0012
Japan

Summary

Drosophila Flamingo is a 7-pass transmembrane cadherin that is necessary for dendritic patterning and axon guidance. How it works at the molecular level and whether homologs of Flamingo play similar roles in mammalian neurons or not have been unanswered questions. Here, we performed loss-of-function analysis using an RNAi system and organotypic brain slice cultures to address the role of a mammalian Flamingo homolog, Celsr2. Knocking down Celsr2 resulted in prominent simplification of dendritic arbors of cortical pyramidal neurons and Purkinje neurons, and this phenotype seemed to be due to branch retraction. Cadherin domain-mediated homophilic interaction appears to be required for the maintenance of dendritic branches. Furthermore, expression of various Celsr2 forms elicited distinct responses that were dependent on an extracellular subregion outside the cadherin domains and on a portion within the carboxyl intracellular tail. Based on these findings, we discuss how Celsr2 may regulate dendritic maintenance and growth.

Introduction

Neurons develop dendritic trees that integrate information from synaptic or sensory inputs, and the spatial pattern of dendritic arborization influences neuronal function, for example, by limiting the number and type of inputs, as was shown in studies on retinal ganglion cells (Masland, 2001; Sterling, 1998). Each type of neuron acquires its unique dendritic pattern by controlling

*Correspondence: tuemura@virus.kyoto-u.ac.jp
[5]Present address: RIKEN Brain Science Institute, Hirosawa 2-1, Wako, Saitama 351-0198.
[6]Present address: Graduate School of Biostudies, Oiwake-cho, Kitashirakawa, Sakyo-ku, Kyoto 606-8507.

cytoskeletal reorganization, and the molecular mechanisms underlying these controls involve a number of environmental cues (Cline, 2001; Jan and Jan, 2003; McAllister, 2000; Miller and Kaplan, 2003; Scott and Luo, 2001; Whitford et al., 2002; Wong and Ghosh, 2002). Several molecular signals of the environmental cues have been identified. For example, Notch signaling inhibits the growth of dendrites of cortical pyramidal neurons, presumably in a contact-dependent manner, and secreted proteins that regulate dendrite growth and/or branching include neurotrophins and semaphorin 3A (Furrer et al., 2003; McAllister, 2000; Whitford et al., 2002). Compared with these molecules, another protein that has been much less characterized at the molecular level is the 7-pass transmembrane cadherin Flamingo (also designated as Starry night) in *Drosophila* (Chae et al., 1999; Usui et al., 1999).

Seven-pass transmembrane cadherins constitute an evolutionarily conserved subfamily of the cadherin superfamily (Hadjantonakis et al., 1998; Tepass et al., 2000; Usui et al., 1999; Yagi and Takeichi, 2000). Their extracellular regions consist of cadherin repeats and other motifs that are suggestive of protein-protein interaction, and sequences of transmembrane domains show similarity to those of the secretin-receptor family of G protein-coupled receptors (Figure 1A). Phenotypic analysis of *flamingo* (*fmi*) mutants has shown pleiotropic roles of Fmi in controlling epithelial and neuronal cell morphogenesis. In epithelia, Fmi regulates planar cell polarity (PCP) as a component of a noncanonical Frizzled signaling pathway (PCP pathway). At least one aspect of this role of Fmi is the anchoring of signaling molecules that belong to this pathway at intercellular junctions, which occurs via homophilic binding (Eaton, 2003; Mlodzik, 2002; Strutt, 2003; Uemura and Shimada, 2003; Usui et al., 1999; Veeman et al., 2003). In neural development of *Drosophila*, Fmi was shown to be required for controlling the extension and/or guidance of dendrites and axons of multiple types of neurons (Gao et al., 1999, 2000; Grueber et al., 2002; Lee et al., 2003; Reuter et al., 2003; Senti et al., 2003; Sweeney et al., 2002). Whereas Fmi operates in the PCP pathway in epithelia, Fmi-dependent dendritic and axonal outgrowth appears to occur separate from the PCP pathway (Gao et al., 2000; Lee et al., 2003; Senti et al., 2003), and the molecular function of Fmi in neurons is largely unknown.

Three mammalian homologs of *fmi*, designated as *Celsr1*, *-2*, and *-3*, are differentially expressed in the developing CNS in the mouse (Formstone and Little, 2001; Shima et al., 2002; Tissir et al., 2002), and Celsr2 protein is distributed in dendrites and axons of embryonic and postnatal neurons such as hippocampal and cortical pyramidal cells and Purkinje neurons (Shima et al., 2002). In this study, we combined organotypic brain slice cultures and DNA vector-based RNA interference (RNAi) technology (Brummelkamp et al., 2002; Miyagishi and Taira, 2002; Paddison et al., 2002; Sui et al., 2002) to perform loss-of-function analysis of Celsr2 in terms of dendritic morphogenesis. siRNA expression caused
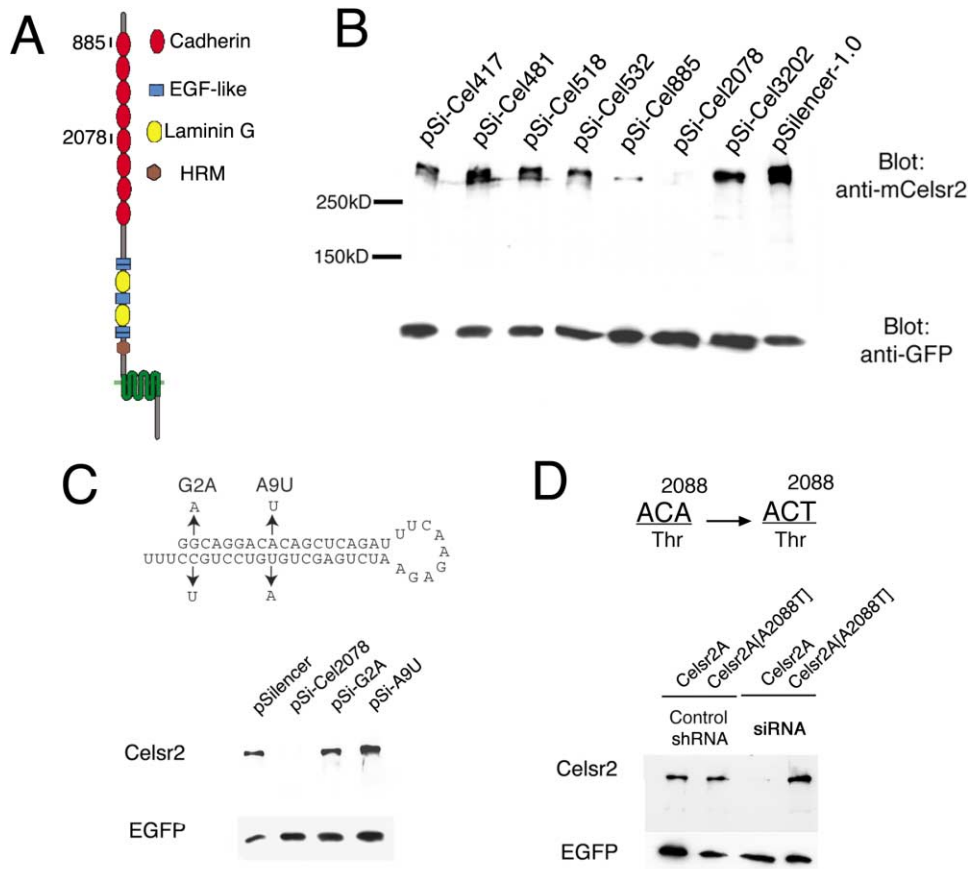
Figure 1. Sequence-Specific Silencing of *Celsr2* by a Plasmid Expressing shRNA

(A) Schematic representation of Celsr2A protein (2920 amino acids in length). The extracellular region includes eight tandemly repeated cadherin domains, five EGF-like domains, two laminin G domains, and a hormone receptor domain (HRM). Positions of target sequences of two siRNA molecules are indicated.

(B) 293T cells were cotransfected with each shRNA-expressing plasmid or the vector (pSilencer1.0), a mouse Celsr2A expression plasmid, and an EGFP plasmid. Lysates of transfected cells were blotted with antibodies to mCelsr2 (top) and GFP (bottom). The number in each plasmid name indicates the first nucleotide number of shRNA in the *Celsr2* sequence.

(C) shRNA product of pSi-Cel2078 and introduced single base pair substitutions (G2A and A9U). pSilencer1.0, pSi-Cel2078, and either of the mutated plasmids (pSi-G2A or pSi-A9T) were used in the cotransfection assay as described in (B).

(D) In *Celsr2A^{A2088}*, the 2088th nucleotide of *Celsr2A* cDNA was substituted from A to T (top). *Celsr2A* or *Celsr2A^{A2088T}* expression plasmid was coexpressed with either pSi-G2A (lanes of control shRNA) or pSi-Cel2078 (lanes of siRNA) and analyzed as in (B) (bottom).

severe simplification of dendritic arbors of cortical pyramidal cells and Purkinje neurons. This phenotype was rescued by coexpressing a siRNA-resistant form of *Celsr2*, indicating that the simplification phenotype was most likely due to knockdown of *Celsr2*. Furthermore, we performed two types of structure-function analysis of Ceslr2: in one analysis, we investigated which domain was necessary for the rescue activity, and in the other, we examined whether the expression of several mutant forms of Ceslr2 by themselves would result in malformation of dendritic trees when slices were cultured for a longer period. On the basis of our results, we discuss how Celsr2 controls dendritic morphology.

Results

Sequence-Specific Silencing of *Celsr2* by RNAi

We attempted to knock down expression of the target gene, *Celsr2*, by expressing small hairpin RNA (shRNA) that was subsequently converted into small interference

RNA (siRNA) in cells. To find a RNA sequence that would be effective in silencing of *Celsr2*, we first made plasmids that synthesized shRNA of different target recognition sequences and then coexpressed each shRNA with Celsr2 and EGFP in 293T cells (see details in the Experimental Procedures). Out of the seven shRNA-expressing plasmids that were examined, transfection with either of two of these plasmids (pSi-Cel885 and pSi-Cel2078) strongly reduced the level of Celsr2 protein, whereas neither of these plasmids affected the level of a control protein, EGFP (Figure 1B). The RNA product of pSi-Cel2078 in cells (designated as siRNA2078 or simply the siRNA hereafter) exhibited a more potent effect than that of pSi-Cel885 (designated as siRNA885); therefore, pSi-Cel2078 was mostly used in subsequent experiments. We had found that two splice variants were generated from *Celsr2* in the mouse nervous system and that one of them lacked exon 31, which encodes a middle portion within the carboxyl intracellular tail (see Supplemental Figure S1 at http://www.developmentalcell.

com/cgi/content/full/7/2/205/DC1). We designated proteins that were translated from the longer and shorter splice variants as Celsr2A and Celsr2B, respectively. All of the shRNA molecules were designed to target both splice variants (Figure 1A).

The results of two experiments that are described below show that the silencing activity of siRNA2078 was abolished by a single nucleotide mismatch between the siRNA and *Celsr2*; thus the silencing was highly sequence specific. In the first experiment, single base pair substitutions were introduced into the siRNA sequence, and neither of the resultant plasmids (pSi-G2A and pSi-A9U) decreased the level of Celsr2 protein when used for transfection (Figure 1C). This result indicates that RNA products of these two plasmids did not possess silencing activity. In most of our transfection experiments using brain slices, transfection with pSi-G2A served as a negative control, and its shRNA was designated as the control shRNA. In the second experiment, *Celsr2A* cDNA was mutated to generate *Celsr2A*^{A2088T}, which had a silent point mutation within the target sequence of siRNA2078 (Figure 1D, top). Then, we examined if siRNA2078 expression would reduce the level of the protein that was made from *Celsr2A*^{A2088T}. In contrast to the potent and reproducible silencing effect of siRNA2078 on the wild-type *Celsr2A* expression, *Celsr2A*^{A2088T}-derived protein was detected at a level comparable to that in the negative control experiment (Figure 1D, bottom). Therefore, *Celsr2A*^{A2088T} expression appeared to be insensitive to siRNA2078, and so this mutated *Celsr2A* was used in our subsequent attempts to recover siRNA-induced dendritic phenotypes (see below).

Dendritic Simplification of Pyramidal Cells
To investigate the role of Celsr2 in dendritic morphology, we expressed siRNA2078 or the control shRNA together with EGFP in neurons in organotypic brain slices by biolistic transfection. Plasmids were used for cotransfection of a large number of pyramidal neurons in cortical slices prepared from postnatal day 8 (P8) rats. We fixed the slices 3 days after transfection and observed fluorescent pyramidal neurons (Figures 2A–2C). For ease of evaluation of dendritic morphology, we focused on pyramidal neurons in layer V, which have well-developed dendrites.

Neurons that expressed the control shRNA looked morphologically similar to those expressing only EGFP (cf. Figures 2A and 2C). In contrast, siRNA2078-expressing pyramidal cells had visibly less complex dendritic morphologies than the two controls, and this effect appeared to be due to fewer and shorter primary branches (Figure 2B). The effect of the siRNA or the control shRNA on dendritic shape was quantified as shown in Figures 2D–2G. Expression of the siRNA, but not that of the control shRNA, caused statistically significant reductions in the lengths of apical dendrites and longest basal dendrites and in the number of terminals of the basal dendrites as well (Figures 2D–2F). We further performed Sholl analysis, in which the number of dendrites crossing concentric circles was counted, and thus it should be noted that the dendritic complexity that was quantified by Sholl plots reflected the number, the length, and the arborization of branches (see details in the Experimental

Procedures). The plots revealed a marked decrease in the complexity of basal dendrites of siRNA-expressing cells compared with that of the control neurons (Figure 2G). Expression of another siRNA (siRNA885) resulted in a milder but qualitatively similar effect (data not shown). All of the above quantitative data show that siRNA expression targeting *Celsr2* led to dendritic simplification. This phenotype was seen in pyramidal cells, not only in layer V but also in the other layers (data not shown).

Phenotypic Rescue by siRNA-Resistant *Celsr2A*
Distinct effects of siRNA2078 and the control shRNA suggested that a reduction in the Celsr2 level caused the decrease in dendritic complexity. To test this hypothesis, we tried to "rescue" the siRNA-induced phenotype by coexpressing the target gene together with the siRNA. For this purpose, gold particles for transfection were coated with a mixture of expression plasmids of Celsr2A, EGFP, and the siRNA. When plasmids of the wild-type *Celsr2A* cDNA and the siRNA were used for the cotransfection, pyramidal neurons formed arbors as poor as those that expressed the siRNA alone (Figure 3A). In contrast, neurons that were cotransfected with plasmids of *Celsr2A*^{A2088T} and the siRNA produced longer primary branches, and dendritic arbors appeared to have developed as well as those of the cells that expressed EGFP alone (Figure 3B). In all these transfection experiments, dendritic complexity was quantified by Sholl analysis, and statistical comparison of those plots confirmed the phenotypic rescue by siRNA-resistant *Celsr2A*^{A2088T} but not by the wild-type *Celsr2A* (Figure 3C). This result supports the above-mentioned data showing that silencing *Celsr2* caused the decrease in dendritic complexity.

Malformation of Purkinje Dendrites
To examine whether Celsr2 may play an important role in dendritic morphogenesis of other types of neurons that express Celsr2, we used the siRNA-expressing plasmid for transfection of Purkinje neurons in slices that were prepared from P10 rats. Purkinje neurons were not readily transfected with plasmids, and consequently the total sample size was smaller than that of pyramidal neurons (see details in the Experimental Procedures). Nevertheless, we found that the Purkinje neurons expressing the siRNA formed much simpler and less organized dendritic trees than those expressing the control shRNA did (Figures 4A and 4B). The siRNA-expressing cells displayed a range of abnormalities that could be grouped into three classes (mild, severe, and extreme) according to the severity of the phenotypes. Expression of the control shRNA did not appear to affect dendritic shape when morphologies of cells expressing both the shRNA and EGFP were compared with those expressing EGFP alone (data not shown).

The siRNA-induced malformation of Purkinje dendrites appeared to be recovered by coexpressing *Celsr2A*^{A2088T} with the siRNA (Figure 4C). To analyze the morphological complexity quantitatively, we performed Strahler analysis (Berry and Bradley, 1976) (Figures 4D and 4E and Table 1). Values of individual Strahler orders were significantly reduced in the siRNA-expressing cells, whereas there was no statistically significant difference between
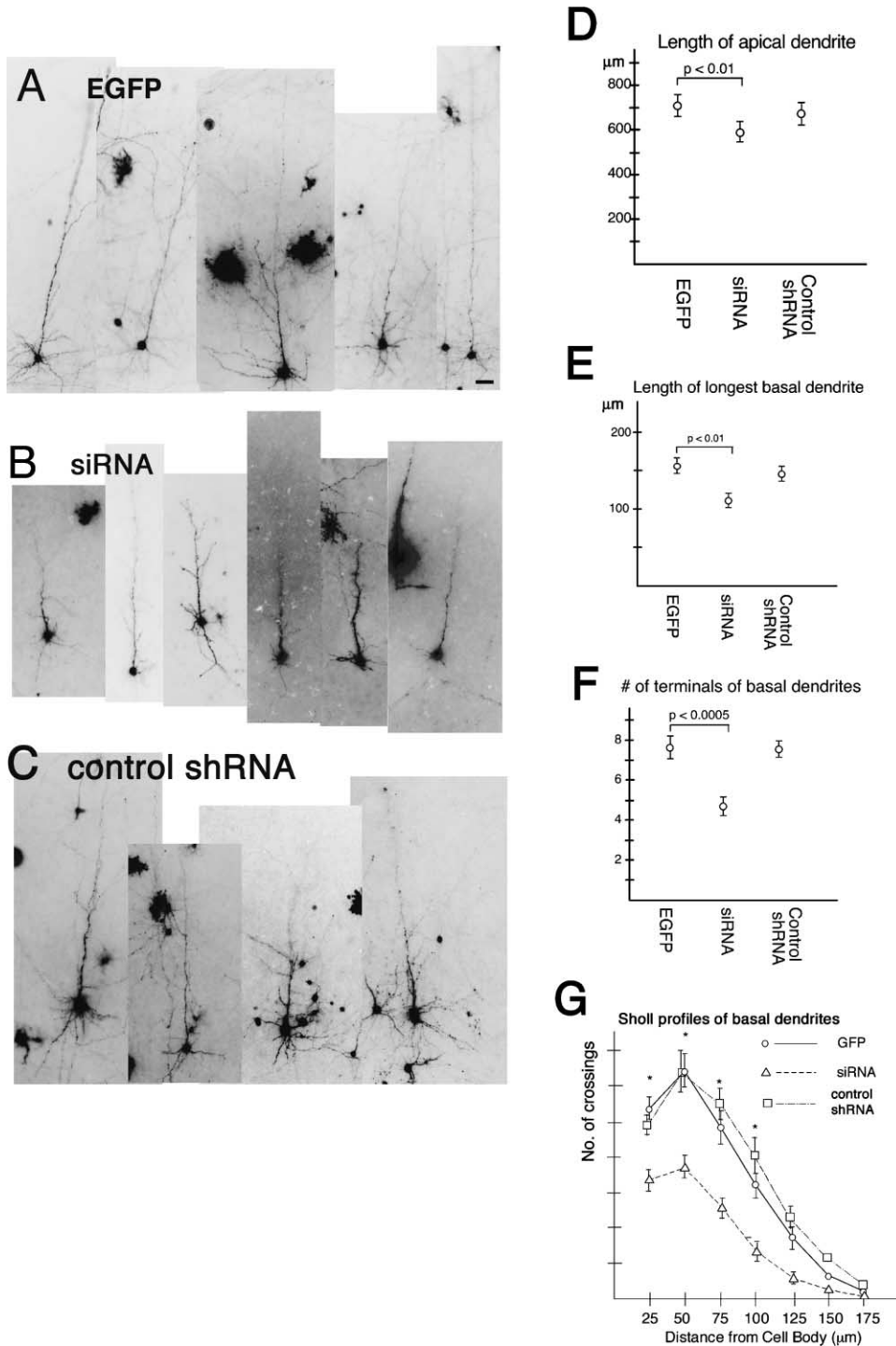
Figure 2. Expression of the siRNA Resulted in Dendritic Simplification of Cortical Pyramidal Neurons

(A–C) Images of layer V pyramidal neurons expressing EGFP (A), the siRNA (B), or control shRNA (C) at 3 DIV after transfection. Scale bar, 50 μm.

(D–G) Quantification of dendritic length (D and E), the number of basal dendritic terminals per cell (F), and complexity (G). (D) Length of apical dendrites was reduced in neurons expressing siRNA (586 ± 30 μm) when compared with that of those expressing EGFP (700 ± 30 μm; $p < 0.01$), whereas expression of the control shRNA (642 ± 30 μm) did not result in a statistically significant difference from EGFP expression ($p = 0.17$). (E) Length of the longest basal dendrites was reduced in neurons expressing siRNA (117 ± 11 μm), compared with those expressing EGFP (156 ± 11 μm; $p < 0.01$), and there was no statistically significant difference between cells expressing control shRNA (144 ± 10 μm) and those expressing EGFP ($p = 0.46$). (F) The number of terminals of basal dendrites per cell decreased in cells expressing siRNA (4.7 ± 0.46), compared with that of those expressing EGFP (7.6 ± 0.48; $p < 0.0005$), whereas the difference between cells expressing control shRNA (7.48 ± 0.44) and those expressing EGFP was not significant ($p = 0.85$). (G) Sholl profiles for basal dendrites revealed a reduction in the number of dendrite crossings when siRNA was used (25–100 μm distance from cell body; $*p < 0.001$). $n = 31–41$ in (D)–(G).
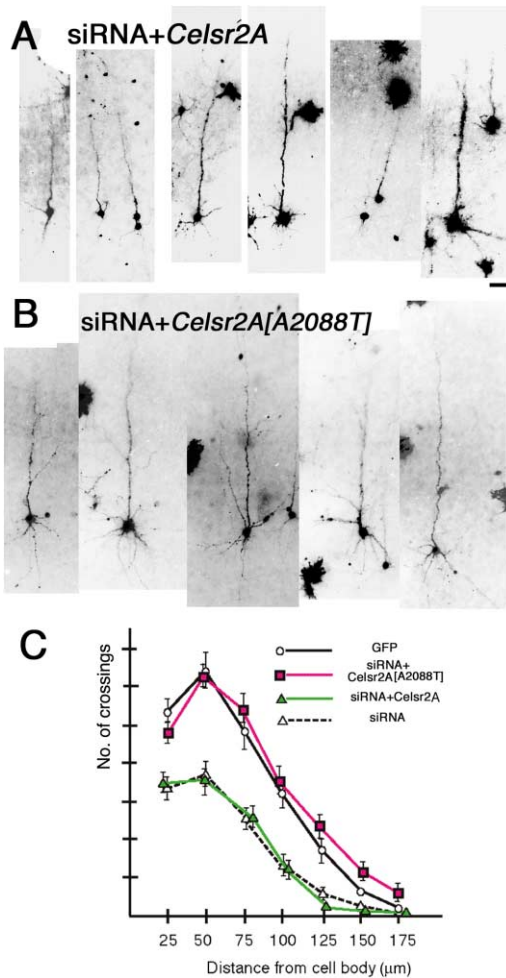
Figure 3. The Dendritic Simplification Phenotype Was Rescued by Expression of siRNA-Resistant Celsr2A[A2088T] but Not by that of the Wild-Type Gene

(A and B) Pyramidal neurons were cotransfected with the siRNA plasmid and an expression plasmid of either the wild-type Celsr2A (A) or Celsr2A[A2088T] (B), and images were taken 3 DIV following transfection. n = 31 for each coexpression experiment. Scale bar, 50 μm.
(C) Sholl profiles for basal dendrites in cotransfection experiments in (A) and (B) are given in Figure 2G.

the values of the control shRNA-expressing cells and those of the "rescued" cells (Table 1). Our results on the Purkinje neurons support our above conclusion that knocking down Celsr2 caused the dendritic phenotype.

Next, we sought to substantiate a decrease in the level of endogenous Celsr2 in neurons that were transfected with the siRNA-expressing plasmid. For this purpose, we stained brain slices for Celsr2 and assessed whether or not expression of the siRNA reduced the immunoreactivity in the neurons. One major technical difficulty of this approach was that slices were not stained evenly, probably because antibodies did not adequately penetrate into the 400 μm thick slices that were used. Nonetheless, our estimation pointed to a decrease in the Celsr2 signal in siRNA plasmid-transfected Purkinje neurons compared with that in nontransfected cells (see details in Supplemental Figure S2 and
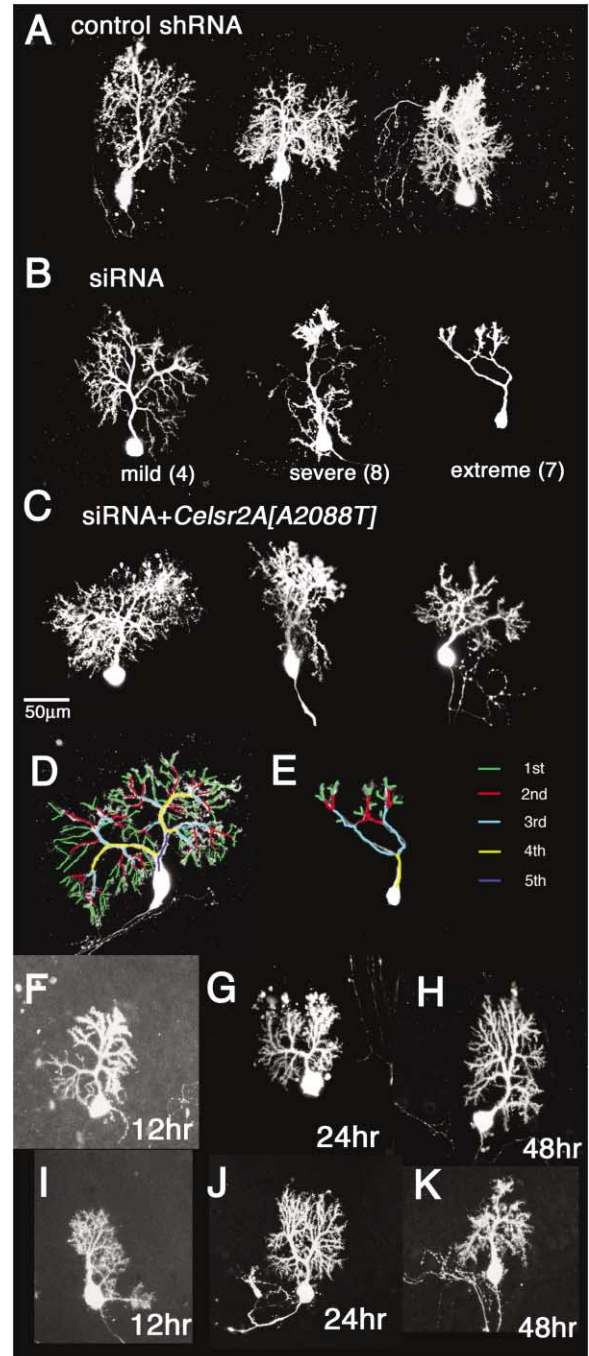

Figure 4. Dendritic Malformation of Purkinje Neurons by siRNA Expression

(A) Images of Purkinje neurons expressing the control shRNA (n = 7).
(B) Images of a total of 19 siRNA-expressing Purkinje neurons were captured, and their morphologies were grouped into three classes (mild, severe, and extreme). The cell number of each phenotypic class is indicated.
(C) Images of Purkinje neurons that expressed both the siRNA and Celsr2[A2088T] (n = 8).
(D and E) Dendritic branches of a control shRNA-expressing cell (D) and one example of the "extreme" class (E) were colored according to the Strahler order for quantification of the complexity (see details in the Experimental Procedures and also Table 1).
(F–K) Purkinje neurons, which had been transfected with control shRNA plasmid (F–H) or siRNA plasmid (I–K) were fixed 12 hr (F and I), 24 hr (G and J), or 48 hr (H and K) after transfection. Scale bar, 50 μm.

Table 1. Quantification of the Dendritic Tree Complexity by the Strahler Method

Culture after transfection	Transfection	Strahler Order				
		First	Second	Third	Fourth	Fifth
12 hr	Control shRNA (n = 9)	52.0 (35–85)	16.7 (11–27)	5.11 (3–8)	2.11 (1–4)	0.77 (0–1)
	siRNA (n = 7)	45.0 (38–70)	16.7 (12–28)	3.86 (3–6)	1.71 (1–3)	0.57 (0–1)
24 hr	Control shRNA (n = 7)	66.4 (42–89)	23.0 (18–36)	7.57 (5–10)	2.71 (2–3)	0.86 (0–1)
	siRNA (n = 9)	40.1 (25–86)	14.5 (5–32)	4.78 (2–9)	1.89 (1–3)	0.44 (0–1)
48 hr	Control shRNA (n = 8)	68.4 (38–93)*	24.5 (15–38)*	8.0 (4–13)*	2.5 (2–3)*	0.86 (0–1)
	siRNA (n = 10)	30.1 (20–42)	9.0 (4–18)	2.30 (1–5)	0.80 (1–2)	0.30 (0–1)
72 hr	Control shRNA (n = 7)	70.7 (38–114)*	24.7 (17–45)*	6.57 (4–12)*	2.14 (1–3)*	0.86 (0–1)
	siRNA (n = 19)	35.4 (20–83)	10.6 (3–24)	2.42 (1–7)	0.526 (0–2)	0.053 (0–1)
	siRNA + Celsr2 [A2088T] (n = 8)	61.0 (40–105)*	23.7 (18–38)*	5.63 (3–8)*	2.38 (2–3)*	0.88 (0–1)

Purkinje cells were transfected with indicated plasmids, and then numbers of dendrites of individual Strahler order were counted at 12, 24, 48, and 72 hr after transfection. In each pair of parentheses is shown a range of the number of branches that are given each Strahler order. The numbers to the left of the parentheses indicate average values. Within each Strahler order, the range of the branch number of siRNA-expressing Purkinje neurons was compared with that of control shRNA-expressing cells or that of cells expressing both the siRNA and $Celsr2A^{A2088T}$ and assessed by use of the Wilcoxon test (*p < 0.01).

its legend at http://www.developmentalcell.com/cgi/content/full/7/2/205/DC1).

The RNAi Phenotype Seemed to Be Due to Dendritic Retraction

The knockdown phenotypes of the two types of neurons at 3 days after transfection could be interpreted as being due to either growth retardation or retraction of already formed dendritic arbors. To distinguish these two possibilities, we monitored dendritic growth in our slice cultures at multiple time points before the third day. Cerebellar slices were transfected with an EGFP plasmid, and then images of Purkinje dendrites were captured 12 hr, 24 hr, or 48 hr later (Figures 4F–4K and Table 1). It seemed that Purkinje neurons had already developed their dendritic trees to some extent at 12 hr or 24 hr after transfection, and they showed a slight increase in the number of branch terminals during the subsequent culture periods (Table 1). Dendritic morphologies of siRNA-expressing cells looked distinguishable to those of control cells at 48 hr but not at 12 hr or 24 hr (Figures 4F–4K). Strahler analysis showed that dendritic complexity of siRNA-expressing cells was comparable to that of the control shRNA-expressing cells at 12 hr and 24 hr; in contrast, the numbers of individual Strahler orders in siRNA-expressing cells were significantly less than those of the control at 48 hr (Table 1).

Because of the technical difficulty in transfecting Purkinje neurons, the number of cells examined was low, and the spread of the data was wide. Nonetheless, all of the above results suggested our contention that gene silencing of *Celsr2* caused dendritic retraction of Purkinje neurons. In contrast to Purkinje neurons, cortical pyramidal neurons did not start emitting green fluorescence that was strong enough to allow visualization of branch terminals until the second day following the transfection with the EGFP plasmid. Therefore, it was difficult to draw a conclusion concerning the cellular basis of the phenotype of pyramidal neurons by using our approach.

Domains that Were Required for the Rescue

To gain mechanistic insight into the molecular function of Celsr2, we addressed whether or not the siRNA-induced phenotype could be rescued by coexpressing each of several deletion forms of Celsr2A (Figure 5). Expression constructs that contained the target recognition sequence of the siRNA were made from $Celsr2A^{A2088T}$ cDNA. We dissected the extracellular region of Celsr2 into two subregions: a string of tandemly repeated cadherin domains (CR) and the more membrane-proximal subregion that contains motifs such as EGF-like domains, laminin G domains, and a hormone receptor domain (HRM) (Figure 1A). This membrane-proximal subregion was designated as the EGF-HRM region. Expression of ΔEGFHRM-A, an A form without the EGF-HRM region, rescued the knockdown phenotypes of pyramidal neurons and Purkinje neurons (Figure 5A), whereas ΔCR-A and ΔEX-A, in which the cadherin domains were totally deleted, did not (Figures 5B and 5C, respectively).

We also studied two forms that had modified intracellular or transmembrane domains. One was Celsr2B, which lacked part of the carboxyl intracellular tail that includes residues conserved among the Fmi/Celsr family (Supplemental Figure S1 at http://www.developmentalcell.com/cgi/content/full/7/2/205/DC1), and the other was Ex-1TM, in which the entire 7-pass transmembrane domain and the carboxyl tail were substituted with the single-pass domain of N-cadherin. Neither Celsr2B nor Ex-1TM recovered the effect of the siRNA (Figures 5D and 5E). These results of our structure-function analysis show that the cadherin repeats as well as the carboxyl intracellular portion were required for rescuing the siRNA-induced dendritic malformation. In all of our attempts to rescue the knockdown phenotypes described here, we observed dendritic morphology at 3 days in vitro (DIV). In parallel with the coexpression of each Celsr2 form with the siRNA, we also expressed each form alone and found that expression of any form by itself did not give rise to statistically significant morphological effects when compared with the EGFP expression at 3 DIV (data not shown, but see below).

We previously showed that *Drosophila* Flamingo (Fmi) has a homophilic cell binding property when expressed in S2 cells (Usui et al., 1999). So, we investigated whether
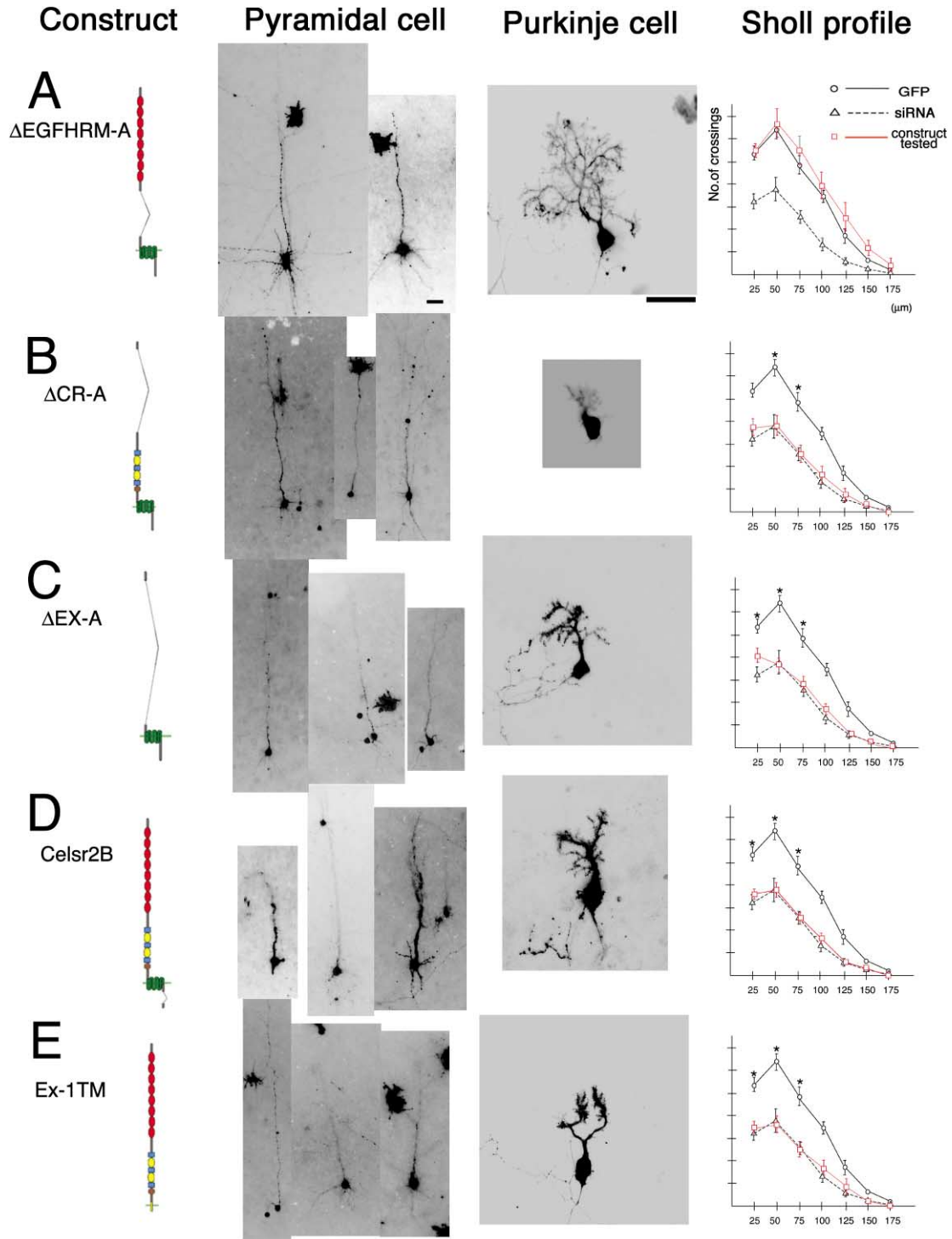
Construct	Pyramidal cell	Purkinje cell	Sholl profile
A ΔEGFHRM-A			
B ΔCR-A			
C ΔEX-A			
D Celsr2B			
E Ex-1TM			

Figure 5. Domain Deletion Analysis for Rescuing the siRNA-Induced Phenotype

Illustrated at the most left are the following forms of Celsr2: ΔEGFHRM-A (A), ΔCR-A (B), ΔEx (C), Celsr2B (D), and EX-1TM (E). We expressed each form and the siRNA together and examined whether the siRNA-induced phenotype was rescued at 3 DIV after transfection. Representative images of pyramidal neurons and Purkinje neurons are shown. Scale bars, 50 μm. Basal dendrites of pyramidal neurons were analyzed with Sholl profiles (n = 31–40 in [A]–[E]), and * indicates $p < 0.001$. Four or five Purkinje cells were observed for each construct. Four out of four ΔEGFHRM-A-transfected Purkinje cells showed only a "mild" phenotype, whereas almost all cells that had been transfected with other constructs had either a "severe" or "extreme" phenotype.
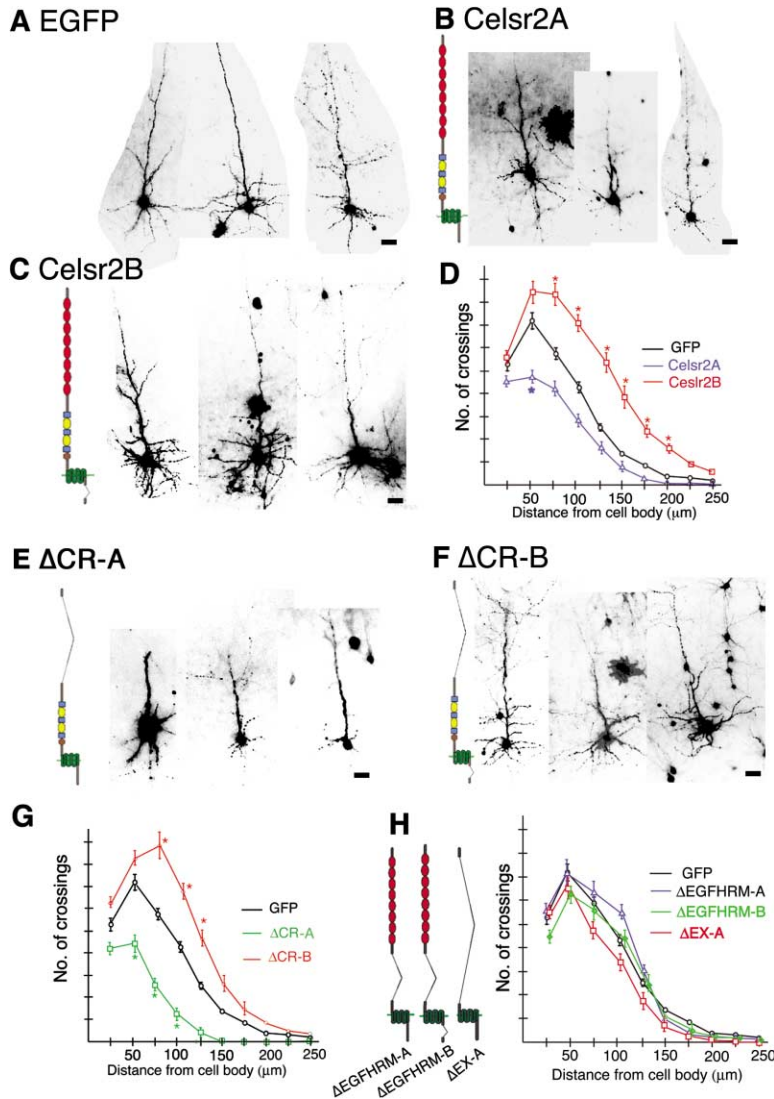
Figure 6. Expression of Each Form Alone Displayed Distinct Responses of Dendritic Morphologies at 6 DIV

(A–C, E, F, and H) Expressed in pyramidal neurons were EGFP or EGFP plus each form, and images were taken at 6 DIV following transfection. Scale bar, 50 μm. (D, G, and H) Complexities of basal dendrites were analyzed and are represented by Sholl profiles. Statistically significant differences, with comparison to the crossing numbers of GFP-expressing cells, are indicated by * (p < 0.001). n = 27–44 for analyses of individual transfection experiments.

several forms of Celsr2 conferred homophilic cell binding to S2 cells or not. Celsr2A, Celsr2B, or ΔEGFHRM-A-expressing S2 cells adhered to each other as Fmi-expressing cells did; on the other hand, cells expressing molecules without cadherin domains did not aggregate (Supplemental Figure S3 at http://www.developmentalcell. com/cgi/content/full/7/2/205/DC1). This result indicates that cadherin repeats of Celsr2 possessed a homophilic binding property and that Celsr2A, Celsr2B, and ΔEGFHRM-A were sorted to the plasma membrane at least in this heterologous system. Thus, it seems less likely that the inability of Celsr2B to rescue the siRNA phenotype was due to mislocalization of the Celsr2B molecules in plasmid-transfected neurons.

Effects of Expression of Individual Forms at 6 DIV

As described above, neurons that overexpressed any form of Celsr2 alone displayed no obvious dendritic phenotype at 3 DIV; however, we did detect effects of the expression at 6 DIV (Figure 6). In our slice cultures,

control pyramidal neurons expressing only EGFP increased in dendritic complexity between 3 DIV and 6 DIV (compare black line in Figure 3C with that in 6D). Depending on extracellular and intracellular structures of the forms to be expressed, at 6 DIV pyramidal neurons exhibited three distinct responses of dendritic morphogenesis when compared to control neurons: no statistically significant difference or either a decrease or an increase in the complexity. Details are described below.

Celsr2A-expressing cells showed a moderate decrease in the dendritic complexity at 6 DIV (compare Figures 6A and 6B and see also 6D). Expression of ΔCR-A caused a similar but much more severe effect (Figures 6E and 6G), which was likely due to retraction of dendritic branches between 3 DIV and 6 DIV. On the other hand, neither of the two forms lacking the EGF-HRM region (ΔEGFHRM-A and ΔEx-A) exhibited such responses (Figure 6H). These findings indicate that the reduction in dendritic complexity caused by expression of Celsr2A or ΔCR-A relied on the EGF-HRM region but not on the cadherin repeats. There was a substantial

difference in the relative extent of the effects between Celsr2A and ΔCR-A (Figures 6B and 6E), suggesting that the cadherin repeats and the EGF-HRM region may exert opposing effects on controlling dendritic complexity.

In contrast to Celsr2A-expressing cells, Celsr2B-expressing cells had more elaborate dendritic arbors than the control cells (compare Figures 6A and 6C and see also 6D). Constructs for ΔCR-B and ΔEGFHRM-B were made from *Celsr2B* cDNA, and promoted elaboration was seen when ΔCR-B, but not ΔEGFHRM-B, was expressed (Figures 6F–6H). These results indicate that the Celsr2B-induced phenotype was dependent on the EGF-HRM region but not the cadherin repeats, exactly as was the Celsr2A-induced phenotype. Our findings in the structure-function analysis suggest the hypothesis that the extracellular region is functionally separable and that the carboxyl tails of Celsr2A and Celsr2B may relay distinct intracellular signals.

Discussion

To study the role of the 7-pass transmembrane cadherin Celsr2 in dendritic morphogenesis, we developed a protocol of loss-of-function analysis using the vector-based RNAi system in conjunction with organotypic brain slice cultures. When maturing neurons were cotransfected with EGFP-expressing plasmids and siRNA-expressing ones, we found dendritic simplification at 3 days following the transfection. Efficient cotransfection with multiple plasmids by the biolistic method allowed us to perform the rescue experiment, for which we designed a mutated version of *Celsr2A* that was refractory to our siRNA by introducing a silent third-codon point mutation within the target sequence. This mutated transgene, but not the wild-type *Celsr2A*, was able to rescue the siRNA-induced dendritic phenotype under the experimental condition that we employed. This result on functional control shows that the phenotype was due to cell-autonomous and temporally restricted gene knockdown. Furthermore, our structure-function analysis indicated which motif in Celsr2A was required for the rescue activity. This whole procedure would be generally applicable to studies where gene function should be addressed under semi-in vivo situations and would be an approach complementary to conditional knockout at the animal level. Recently, a protocol of rescue by a siRNA-resistant gene was applied to show a role of NeuroD in dendritic morphogenesis of cerebellar granule neurons (Gaudilliere et al., 2004).

Gene silencing of *Celsr2* caused a marked decrease in dendritic complexity, which was probably due to dendritic retraction, as suggested for Purkinje neurons on the basis of observation of transfected cells at different fixation points. Ideally, the retraction phenotype should be verified by time-lapse analysis of the same cell in live slices. We speculate that the retraction would also be the case with cortical pyramidal neurons. Dendrites are highly dynamic processes that undergo rapid and continuous extension and retraction (Cline, 2001; Wong and Ghosh, 2002). Therefore, one possible explanation of the net shortening would be more frequent retraction than extension; in other words, the counteraction of

Celsr2A on dendritic shortening could be interpreted as blocking or slowing down retraction rather than promoting extension. This interpretation is based on the fact that two forms of Celsr2 (Celsr2A and ΔEGFHRM-A), which had the rescue activity, did not significantly promote dendritic elongation when each was expressed by itself. Cadherin domains were necessary for the rescue of the siRNA-induced phenotype, and each of the two forms exhibited a cell aggregation activity when expressed in S2 cells. All these findings strongly suggest that Celsr2A-Celsr2A homophilic interaction plays a pivotal role in maintaining dendritic arbors.

Where does such homophilic interaction occur? Because Celsr2 is distributed on both dendrites and axons, the homophilic binding could take place at axodendritic and dendrodendritic contacts. In the cerebellum, it is suggested that normal dendritic development of Purkinje neurons require inputs from their major presynaptic partners, the granule cells (Altman and Bayer, 1997; Hirai and Launey, 2000; McAllister, 2000). Contacts between parallel fibers (axons of granule cells) and dendrites of Purkinje neurons might have been preserved inside the slices that we prepared. Celsr2-mediated signaling may not be necessarily restricted to axodendritic contact sites and may also occur at dendrodendritic contacts. In fact, Notch signaling, which inhibits growth or causes retraction of dendrites of cortical pyramidal neurons, is postulated to occur when one dendritic branch encounters another (Berezovska et al., 1999; Redmond et al., 2000; Sestan et al., 1999). Further characterization of Celsr2 function at the molecular level is needed to address whether the two signaling pathways, which are mediated through Celsr2 and Notch, work at dendrodendritic contacts in an antagonistic fashion to shape dendritic trees or not.

In contrast to the cadherin domains that were highlighted in the rescue experiment, the results of expressing various domain-deleted forms alone for a longer period (6 days instead of 3 days) revealed the importance of the more membrane-proximal subregion that consists of EGF-like domains, laminin G domains, and a hormone receptor domain (HRM). This EGF-HRM region in Celsr2A was not essential for rescuing the knockdown phenotype but was required for manifestation of dendritic simplification in slices cultured for the longer period. The simplification effect of ΔCR-A, which did not have the cadherin domains, was much more potent than that of Celsr2A. We consider that the easiest interpretation of these findings would be that the EGF-HRM region plays a role separate from that of the cadherin domains and that these two extracellular subregions in Celsr2A exert opposing effects for controlling dendritic complexity. All three motifs in the EGF-HRM region implicate protein-protein interactions. One of these motifs is HRM, which is conserved among extracellular parts of one subfamily of G protein-coupled receptors (GPCRs) for peptide hormones such as secretine and calcitonin (Bockaert and Pin, 1999). Thus, we speculate that the EGF-HRM region may bind to (an) as yet unidentified molecule(s) and that this hypothetical binding leads to retraction of dendrites.

How do our results and interpretations on Celsr2A reconcile with what has been shown or suggested about

roles of other members of the 7-pass transmembrane cadherin family, in particular, Fmi in the *Drosophila* nervous system? Genetic analysis has supported a role of Fmi in restricting dendritic extension in two classes of *Drosophila* neurons: dendritic arborization (da) neurons and mushroom body neurons (Gao et al., 2000; Grueber et al., 2002; Sweeney et al., 2002; Reuter et al., 2003). In *fmi* mutant embryos, dendrites of da neurons in the dorsal region overextend toward the dorsal midline. In the wild-type embryo, dendrites of da neurons extend on the basal surface of the epidermis, and both da neurons and epidermis express Fmi. Curiously, the overshooting phenotype of the mutant can be rescued by *fmi* expression in da neurons (Gao et al., 2000). This result of the rescue experiment is difficult to be explained by a role of Fmi-Fmi homophilic interaction between dendrites and epidermis, and it could raise the possibility of a heterophilic interaction between Fmi and some unknown molecule that restricts dendritic growth (see also the Discussion of Lee et al., 2003). Although extensive structure-function analysis of Fmi remains to be done, one of the loss-of-function *fmi* mutations is a missense mutation in the first EGF motif (Sweeney et al., 2002). What these studies on Fmi suggest is reminiscent of the EGF-HRM-dependent retraction phenotype that is caused by Celsr2A overexpression and may support the functional importance of the EGF-HRM region throughout the 7-pass transmembrane cadherin family.

At a later larval stage of the *fmi* mutant, dendritic terminals of da neurons extend beyond the midline and overlap with those of the contralateral side, whereas in the normal larva terminals that come from contralateral sides avoid each other (Gao et al., 2000). This loss of avoidance in the mutant can be interpreted as being due to defective dendrodendritic communication that is normally mediated by homophilic Fmi interaction (but see also Grueber et al., 2002; Jan and Jan, 2003). If this hypothesis is the case, both the Fmi-Fmi homophilic communication and the Celsr2A-Celsr2A interaction contribute to shaping dendritic arbors, although a defect of each communication resulted in superficially distinct effects. Among mammalian *Celsr* genes, mutant mice of *Celsr1* were isolated (Curtin et al., 2003). *Celsr1* mutants show severe malformations in neural tube and die before birth; however, phenotypes regarding neuronal cell morphology were not reported. In contrast to *Celsr2*, *Celsr1* mRNA is present in the ventricular zone but hardly detected in cortical plate in embryonic and postnatal cerebra (Shima et al., 2002; Tissir et al., 2002).

Celsr2B lacks a portion of the carboxyl intracellular tail of Celsr2A, and its coexpression with the siRNA did not rescue the siRNA-induced phenotype at 3 days following transfection. Nevertheless, expression of Celsr2B by itself increased the dendritic complexity after culturing the slices for 6 days. Although this effect provided a contrast with the outcome of Celsr2A expression, longer expression phenotypes of both Celsr2A and -2B depended on the EGF-HRM region, strengthening its functional importance. The portion of the intracellular tail that is absent from the 2B form includes a stretch of 20 amino acids that are similar among Fmi/Celsr2 members. The distinct effects of the two forms may reflect activation of different downstream pathways, and such a model is reminiscent of isoforms of the EP3

prostaglandin receptor that differ only at their carboxyl terminal tails and couple to different G proteins (Hatae et al., 2002; Namba et al., 1993). Collectively, we would propose that Celsr2 may receive distinct extracellular cues through either homophilic or heterophilic molecular interaction and also activate different intracellular signaling cascades. Future studies should clarify the identities of the heterophilic interaction and downstream components and how each of those multiple signaling pathways is utilized in different contexts of dendritic growth, stabilization, and retraction to shape mature dendritic arbors.

Experimental Procedures

Molecular Biology, Cell Cultures, and Immunoblotting
We used pSilencer 1.0 (Ambion) to express a shRNA that is composed of two complements of 19 nt sequences separated by a 9 nt spacer. We searched 19 nt sequences from *mCelsr2* cDNA according to the instructions of the manufacturer and other studies (Sui et al., 2002): each sequence should be immediately downstream of AA, start with GG, and have about 50% GC contents. Besides these general instructions, we selected 19 nt sequences that were identical to the rat ortholog, because brain slices were made from rats (see below). Uniqueness of individual target sequences was confirmed by a BLAST search. For gene silencing assay, 293T cells were cotransfected with 0.4 μg of shRNA-expressing plasmids (pSi-shRNA), 0.4 μg of HA-tagged mouse *Celsr2* expression plasmid, and 0.05 μg of an *EGFP* plasmid (pCA-EGFP) by means of Effectene Reagent (Qiagen). Three days after transfection, cell lysates were run in 5% or 15% polyacrylamide gels, blotted to PVDF membrane (BioRad), and analyzed with rabbit anti-GFP (Santa Cruz Biotechnology), rabbit anti-HA (Santa Cruz Biotechnology), or mouse anti-mCelsr2. Plasmids expressing mutant forms of *mCelsr2* were made by use of pcDNA3.1 (Invitrogen). For construction of Ex-1TM, the transmembrane region of mouse N-cadherin (721–723 amino acids) was fused to the extracellular region of Celsr2. For aggregation assays using S2 cells, pUAST-based expression plasmids of various forms of Celsr2 were constructed, and S2 cells were cotransfected with each of those plasmids, *actin5C-GAL4* (a gift of Yash Hiromi), and pUAST-EGFP to S2 cells. Cell aggregation assays were performed basically as described (Oda et al., 1994).

Preparation of Rat Organotypic Slice Cultures
Wistar rat pups were decapitated, and their brains were dissected and sliced in cold HBSS with a vibratome. P8 cerebra were sliced coronally at a 350 μm thickness, and slices that included somatosensory cortex were used for subsequent cultures, whereas P10 cerebella were sliced sagittally at a 400 μm thickness. Slices were transferred onto Millicell-CM (Millipore) and cultured at the air-media interface under the conditions of 5% CO_2 at 37°C (Stoppini et al., 1991). Cerebral slices were cultured in a medium essentially as described before (Nakayama et al., 2000), supplemented with 6.5 g/l glucose. The medium for cerebellar slices was previously reported (Tanaka et al., 2003). Each medium was changed once every 3 days.

Biolistic Transfection
We used Helios Gene Gun system (BioRad) for preparation of and transfection with DNA-coated gold particles. Particle preparation was performed according to the manufacturer's instructions with some modifications (T. Inoue and T. Ikegami, personal communication). Briefly, plasmids were purified twice by $CsCl_2$ density equilibrium centrifugation. In knockdown or overexpression experiments, pCA-EGFP and a desired expression plasmid were mixed at a weight ratio of 1:1. In rescue experiments, pCA-EGFP, pSi-Cel2078, and one of the given constructs were mixed at the weight ratio of 5:4:1, respectively. Thirty micrograms of the DNA mixture (1 μg/μl) and 15 μg of gold particles (1.0 μm in diameter) were mixed with 30 μl of 50 mM spermidine dissolved in ethanol. This DNA-particle mixture was precipitated by adding 30 μl of 2 M $CaCl_2$ gradually and washed three times with dehydrated ethanol for organic chemistry use

(Wako Pure Chemical Industries). Then, the DNA-coated particles were suspended in 1.25 ml of 20 μg/ml polyvinylpyrrolidone in ethanol and loaded into tefzel tubing. After particles were precipitated, the ethanol was removed, and the tube was then dried and cut into appropriate lengths. Plasmid-coated particles were propelled into slices with a rapid helium burst of 200 psi, and the particles exited the gun 2–3 cm above the slices.

Biolistic transfection was performed at 16–18 hr and within 3 hr after in vitro cultures of cerebral slices and cerebellar slices, respectively, had been prepared. Under the experimental conditions employed, images of two to eight pyramidal neurons in layer V could be collected per cerebral slice, and only one to two Purkinje neurons in a total of three to four cerebellar slices were transfected per experiment. High efficiency of cotransfection was confirmed by the fact that almost all cells that had been transfected with a mixture of EGFP plasmids and DsRed plasmids emitted both green and red fluorescence. As a positive control of biolistic transfection and expression of incorporated genes, we transfected cortical pyramidal cells with an EGFP plasmid and an active RhoA (RhoA[V14]) plasmid and found marked simplification of dendritic trees, as previously reported for hippocampal pyramidal neurons (data not shown).

Image Analysis and Quantification

Slices were fixed with 2% paraformaldehyde and 4% sucrose in PBS for 1.5 hr. Images of individual pyramidal cells in layer V were captured by using a MZFL3 fluorescence stereomicroscope (Leica) attached to an Axiocam CCD system (Zeiss). To obtain the Sholl profiles of dendritic arbors (Sholl, 1953), we superimposed concentric circles with increasing radii of 25 μm on each image, with the center of the circles placed on the cell body. Then, the number of dendrites crossing each circle was counted and plotted. Welch's t test was performed unless stated otherwise in the figure legends. Cerebellar slices were mounted on slide glasses, and individual Purkinje neurons were imaged by using LSM510 confocal microscopy (Zeiss). The complexity of the Purkinje neurons was quantified by the Strahler method (Berry and Bradley, 1976). In this method, every branch is given an order as follows: Terminal branches are given the first order. When two "n" order branches meet, an "n + 1" order is created, whereas an "n + 1" order meeting with an "n" remains "n + 1." Each Purkinje neuron was manually colored according to the orders of branches.

Acknowledgments

References

Altman, J., and Bayer, S.A. (1997). Development of the Cerebellar System (Boca Raton, FL: CRC Press).

Berezovska, O., McLean, P., Knowles, R., Frosh, M., Lu, F.M., Lux, S.E., and Hyman, B.T. (1999). Notch1 inhibits neurite outgrowth in postmitotic primary neurons. Neuroscience 93, 433–439.

Berry, M., and Bradley, P. (1976). The growth of the dendritic trees of Purkinje cells in the cerebellum of the rat. Brain Res. 112, 1–35.

Bockaert, J., and Pin, J.P. (1999). Molecular tinkering of G protein-coupled receptors: an evolutionary success. EMBO J. 18, 1723–1729.

Brummelkamp, T.R., Bernards, R., and Agami, R. (2002). A system for stable expression of short interfering RNAs in mammalian cells. Science 296, 550–553.

Chae, J., Kim, M.J., Goo, J.H., Collier, S., Gubb, D., Charlton, J., Adler, P.N., and Park, W.J. (1999). The Drosophila tissue polarity gene starry night encodes a member of the protocadherin family. Development 126, 5421–5429.

Cline, H.T. (2001). Dendritic arbor development and synaptogenesis. Curr. Opin. Neurobiol. 11, 118–126.

Curtin, J.A., Quint, E., Tsipouri, V., Arkell, R.M., Cattanach, B., Copp, A.J., Henderson, D.J., Spurr, N., Stanier, P., Fisher, E.M., et al. (2003). Mutation of Celsr1 disrupts planar polarity of inner ear hair cells and causes severe neural tube defects in the mouse. Curr. Biol. 13, 1129–1133.

Eaton, S. (2003). Cell biology of planar polarity transmission in the Drosophila wing. Mech. Dev. 120, 1257–1264.

Formstone, C.J., and Little, P.F. (2001). The flamingo-related mouse Celsr family (Celsr1–3) genes exhibit distinct patterns of expression during embryonic development. Mech. Dev. 109, 91–94.

Furrer, M.P., Kim, S., Wolf, B., and Chiba, A. (2003). Robo and Frazzled/DCC mediate dendritic guidance at the CNS midline. Nat. Neurosci. 6, 223–230.

Gao, F.B., Brenman, J.E., Jan, L.Y., and Jan, Y.N. (1999). Genes regulating dendritic outgrowth, branching, and routing in Drosophila. Genes Dev. 13, 2549–2561.

Gao, F.B., Kohwi, M., Brenman, J.E., Jan, L.Y., and Jan, Y.N. (2000). Control of dendritic field formation in Drosophila: the roles of flamingo and competition between homologous neurons. Neuron 28, 91–101.

Gaudilliere, B., Konishi, Y., de la Iglesia, N., Yao, G., and Bonni, A. (2004). A CaMKII-NeuroD signaling pathway specifies dendritic morphogenesis. Neuron 41, 229–241.

Grueber, W.B., Jan, L.Y., and Jan, Y.N. (2002). Tiling of the Drosophila epidermis by multidendritic sensory neurons. Development 129, 2867–2878.

Hadjantonakis, A.K., Formstone, C.J., and Little, P.F. (1998). mCelsr1 is an evolutionarily conserved seven-pass transmembrane receptor and is expressed during mouse embryonic development. Mech. Dev. 78, 91–95.

Hatae, N., Sugimoto, Y., and Ichikawa, A. (2002). Prostaglandin receptors: advances in the study of EP3 receptor signaling. J. Biochem. (Tokyo) 131, 781–784.

Hirai, H., and Launey, T. (2000). The regulatory connection between the activity of granule cell NMDA receptors and dendritic differentiation of cerebellar Purkinje cells. J. Neurosci. 20, 5217–5224.

Jan, Y.N., and Jan, L.Y. (2003). The control of dendrite development. Neuron 40, 229–242.

Lee, R.C., Clandinin, T.R., Lee, C.H., Chen, P.L., Meinertzhagen, I.A., and Zipursky, S.L. (2003). The protocadherin Flamingo is required for axon target selection in the Drosophila visual system. Nat. Neurosci. 6, 557–563.

Masland, R.H. (2001). The fundamental plan of the retina. Nat. Neurosci. 4, 877–886.

McAllister, A.K. (2000). Cellular and molecular mechanisms of dendrite growth. Cereb. Cortex 10, 963–973.

Miller, F.D., and Kaplan, D.R. (2003). Signaling mechanisms underlying dendrite formation. Curr. Opin. Neurobiol. 13, 391–398.

Miyagishi, M., and Taira, K. (2002). U6 promoter-driven siRNAs with four uridine 3′ overhangs efficiently suppress targeted gene expression in mammalian cells. Nat. Biotechnol. 20, 497–500.

Mlodzik, M. (2002). Planar cell polarization: do the same mechanisms regulate Drosophila tissue polarity and vertebrate gastrulation? Trends Genet. 18, 564–571.

Nakayama, A.Y., Harms, M.B., and Luo, L. (2000). Small GTPases

Rac and Rho in the maintenance of dendritic spines and branches in hippocampal pyramidal neurons. J. Neurosci. *20*, 5329–5338.

Namba, T., Sugimoto, Y., Negishi, M., Irie, A., Ushikubi, F., Kakizuka, A., Ito, S., Ichikawa, A., and Narumiya, S. (1993). Alternative splicing of C-terminal tail of prostaglandin E receptor subtype EP3 determines G-protein specificity. Nature *365*, 166–170.

Oda, H., Uemura, T., Harada, Y., Iwai, Y., and Takeichi, M. (1994). A *Drosophila* homolog of cadherin associated with armadillo and essential for embryonic cell-cell adhesion. Dev. Biol. *165*, 716–726.

Paddison, P.J., Caudy, A.A., Bernstein, E., Hannon, G.J., and Conklin, D.S. (2002). Short hairpin RNAs (shRNAs) induce sequence-specific silencing in mammalian cells. Genes Dev. *16*, 948–958.

Redmond, L., Oh, S.R., Hicks, C., Weinmaster, G., and Ghosh, A. (2000). Nuclear Notch1 signaling and the regulation of dendritic development. Nat. Neurosci. *3*, 30–40.

Reuter, J.E., Nardine, T.M., Penton, A., Billuart, P., Scott, E.K., Usui, T., Uemura, T., and Luo, L. (2003). A mosaic genetic screen for genes necessary for *Drosophila* mushroom body neuronal morphogenesis. Development *130*, 1203–1213.

Scott, E.K., and Luo, L. (2001). How do dendrites take their shape? Nat. Neurosci. *4*, 359–365.

Senti, K.A., Usui, T., Boucke, K., Greber, U., Uemura, T., and Dickson, B.J. (2003). Flamingo regulates r8 axon-axon and axon-target interactions in the *Drosophila* visual system. Curr. Biol. *13*, 828–832.

Sestan, N., Artavanis-Tsakonas, S., and Rakic, P. (1999). Contact-dependent inhibition of cortical neurite growth mediated by notch signaling. Science *286*, 741–746.

Shima, Y., Copeland, N.G., Gilbert, D.J., Jenkins, N.A., Chisaka, O., Takeichi, M., and Uemura, T. (2002). Differential expression of the seven-pass transmembrane cadherin genes Celsr1–3 and distribution of the Celsr2 protein during mouse development. Dev. Dyn. *223*, 321–332.

Sholl, D.A. (1953). Dendritic organization in the neurons of the visual and motor cortices of the cat. J. Anat. *87*, 387–406.

Sterling, P. (1998). The Synaptic Organization of the Brain, Fourth Edition (New York: Oxford University Press).

Stoppini, L., Buchs, P.A., and Muller, D. (1991). A simple method for organotypic cultures of nervous tissue. J. Neurosci. Methods *37*, 173–182.

Strutt, D. (2003). Frizzled signalling and cell polarisation in *Drosophila* and vertebrates. Development *130*, 4501–4513.

Sui, G., Soohoo, C., Affar el, B., Gay, F., Shi, Y., and Forrester, W.C. (2002). A DNA vector-based RNAi technology to suppress gene expression in mammalian cells. Proc. Natl. Acad. Sci. USA *99*, 5515–5520.

Sweeney, N.T., Li, W., and Gao, F.B. (2002). Genetic manipulation of single neurons in vivo reveals specific roles of flamingo in neuronal morphogenesis. Dev. Biol. *247*, 76–88.

Tanaka, M., Maeda, N., Noda, M., and Marunouchi, T. (2003). A chondroitin sulfate proteoglycan PTPζ /RPTPβ regulates the morphogenesis of Purkinje cell dendrites in the developing cerebellum. J. Neurosci. *23*, 2804–2814.

Tepass, U., Truong, K., Godt, D., Ikura, M., and Peifer, M. (2000). Cadherins in embryonic and neural morphogenesis. Nat. Rev. Mol. Cell Biol. *1*, 91–100.

Tissir, F., De-Backer, O., Goffinet, A.M., and Lambert de Rouvroit, C. (2002). Developmental expression profiles of Celsr (Flamingo) genes in the mouse. Mech. Dev. *112*, 157–160.

Uemura, T., and Shimada, Y. (2003). Breaking cellular symmetry along planar axes in *Drosophila* and vertebrates. J. Biochem. (Tokyo) *134*, 625–630.

Usui, T., Shima, Y., Shimada, Y., Hirano, S., Burgess, R.W., Schwarz, T.L., Takeichi, M., and Uemura, T. (1999). Flamingo, a seven-pass transmembrane cadherin, regulates planar cell polarity under the control of Frizzled. Cell *98*, 585–595.

Veeman, M.T., Axelrod, J.D., and Moon, R.T. (2003). A second canon: Functions and mechanisms of β-catenin-independent Wnt signaling. Dev. Cell *5*, 367–377.

Whitford, K.L., Dijkhuizen, P., Polleux, F., and Ghosh, A. (2002). Molecular control of cortical dendrite development. Annu. Rev. Neurosci. *25*, 127–149.

Wong, R.O., and Ghosh, A. (2002). Activity-dependent regulation of dendritic growth and patterning. Nat. Rev. Neurosci. *3*, 803–812.

Yagi, T., and Takeichi, M. (2000). Cadherin superfamily genes: functions, genomic organization, and neurologic diversity. Genes Dev. *14*, 1169–1180.